Research Article | Vol. 9, No. 1 | 1 Jan 2018 | BIOMEDICAL OPTICS EXPRESS 190
Biomedical Optics EXPRESS

Development of a real-time and quantitative thrombus sensor for an extracorporeal centrifugal blood pump by near-infrared light

DAISUKE SAKOTA,[1,*] TATSUKI FUJIWARA,[2] KATSUHIRO OHUCHI,[3] KATSUYUKI KUWANA,[4] HIROYUKI YAMAZAKI,[5] RYO KOSAKA,[1] MASAHIRO NISHIDA,[1] TOMOHIRO MIZUNO,[2,3] HIROKUNI ARAI,[2] AND OSAMU MARUYAMA[1]

[1]*Health Research Institute, National Institute of Advanced Industrial Science and Technology (AIST), 1-2-1 Namiki, Tsukuba-shi, Ibaraki 305-8564, Japan*
[2]*Department of Cardiovascular Surgery, Tokyo Medical and Dental University Graduate School of Medical and Dental Sciences, 1-5-45 Yushima, Bunkyo-ku, Tokyo 113-8519, Japan*
[3]*Department of Advanced Surgical Technology Research and Development, Tokyo Medical and Dental University, 1-5-45 Yushima, Bunkyo-ku, Tokyo 113-8519, Japan*
[4]*Senko Medical Instrument Mfg. Co., Ltd., 3-23-13 Hongo, Bunkyo-ku, Tokyo 113-0033, Japan*
[5]*Optquest Co., Ltd., 1335 Haraichi, Ageo-shi, Saitama 362-0021, Japan*
**sakota.ao@aist.go.jp*

Abstract: We developed an optical thrombus sensor for a monopivot extracorporeal centrifugal blood pump. In this study, we investigated its quantitative performance for thrombus detection in acute animal experiments of left ventricular assist using the pump on pathogen-free pigs. Optical fibers were set in the driver unit of the pump. The incident light at the near-infrared wavelength of 810 nm was aimed at the pivot bearing, and the resulting scattered light was guided to the optical fibers. The detected signal was analyzed to obtain the thrombus formation level. As a result, real-time and quantitative monitoring of the thrombus surface area on the pivot bearing was achieved with an accuracy of 3.6 ± 2.3 mm^2. In addition, the sensing method using the near-infrared light was not influenced by changes in the oxygen saturation and the hematocrit. It is expected that the developed sensor will be useful for optimal anticoagulation management for long-term extracorporeal circulation therapies.

OCIS codes: (170.0170) Medical optics and biotechnology; (170.1470) Blood or tissue constituent monitoring.

References and links

1. P. M. Eckman and R. John, "Bleeding and thrombosis in patients with continuous-flow ventricular assist devices," Circulation **125**(24), 3038–3047 (2012).
2. S. L. Hervey-Jumper, G. M. Annich, A. R. Yancon, H. J. Garton, K. M. Muraszko, and C. O. Maher, "Neurological complications of extracorporeal membrane oxygenation in children," J. Neurosurg. Pediatr. **7**(4), 338–344 (2011).
3. N. A. Gilotra and G. R. Stevens, "Temporary mechanical circulatory support: a review of the options, indications, and outcomes," Clin. Med. Insights Cardiol. **8**(Suppl 1), 75–85 (2015).
4. K. Shekar, S. D. Gregory, and J. F. Fraser, "Mechanical circulatory support in the new era: an overview," Crit. Care **20**(1), 66 (2016).
5. A. Saffarzadeh and P. Bonde, "Options for temporary mechanical circulatory support," J. Thorac. Dis. **7**(12), 2102–2111 (2015).
6. N. M. Milović, J. R. Behr, M. Godin, C. S. Hou, K. R. Payer, A. Chandrasekaran, P. R. Russo, R. Sasisekharan, and S. R. Manalis, "Monitoring of heparin and its low-molecular-weight analogs by silicon field effect," Proc. Natl. Acad. Sci. U.S.A. **103**(36), 13374–13379 (2006).
7. Y. Nosé, "Hemodialysis patients' deaths in the USA by contaminant suspected heparin originating from China," Artif. Organs **32**(6), 425–426 (2008).
8. A. Khetani, V. S. Tiwari, A. Harb, and H. Anis, "Monitoring of heparin concentration in serum by Raman spectroscopy within hollow core photonic crystal fiber," Opt. Express **19**(16), 15244–15254 (2011).

#306512 https://doi.org/10.1364/BOE.9.000190
Journal © 2018 Received 15 Sep 2017; revised 7 Nov 2017; accepted 7 Dec 2017; published 12 Dec 2017

Biomedical Optics EXPRESS

9. K. A. Solen, S. F. Mohammad, G. L. Burns, G. M. Pantalos, J. Kim, Y. Peng, W. G. Pitt, L. O. Reynolds, and D. B. Olsen, "Markers of thromboembolization in a bovine ex vivo left ventricular assist device model," ASAIO J. **40**(3), M602–M608 (1994).
10. Y. Sankai, T. Tsutsui, T. Jikuya, O. Shigeta, M. Ohta, and T. Mitsui, "Method of noninvasive and continuous hemolysis/thrombogenesis measurement by laser photometry during artificial heart development," ASAIO J. **43**(5), M686 (1997).
11. S. Oshima and Y. Sankai, "Development of optical sensing system for noninvasive and dynamic monitoring of thrombogenic process," ASAIO J. **56**(5), 460–467 (2010).
12. Y. Asakura, A. Sapkota, O. Maruyama, R. Kosaka, T. Yamane, and M. Takei, "Relative permittivity measurement during the thrombus formation process using the dielectric relaxation method for various hematocrit values," J. Artif. Organs **18**(4), 346–353 (2015).
13. A. Sapkota, T. Fuse, M. Seki, O. Maruyama, M. Sugawara, and M. Takei, "Application of electrical resistance tomography for thrombus visualization in blood," Flow Meas. Instrum. **46**(B), 334–340 (2015).
14. P. Bahrmann, G. S. Werner, G. Heusch, M. Ferrari, T. C. Poerner, A. Voss, and H. R. Figulla, "Detection of coronary microembolization by Doppler ultrasound in patients with stable angina pectoris undergoing elective percutaneous coronary interventions," Circulation **115**(5), 600–608 (2007).
15. D. Russell, K. P. Madden, W. M. Clark, P. M. Sandset, and J. A. Zivin, "Detection of arterial emboli using Doppler ultrasound in rabbits," Stroke **22**(2), 253–258 (1991).
16. D. Sakota, T. Murashige, R. Kosaka, M. Nishida, and O. Maruyama, "Feasibility of the optical imaging of thrombus formation in a rotary blood pump by near-infrared light," Artif. Organs **38**(9), 733–740 (2014).
17. D. Sakota, T. Murashige, R. Kosaka, T. Fujiwara, M. Nishida, and O. Maruyama, "Real-time observation of thrombus growth process in an impeller of a hydrodynamically levitated centrifugal blood pump by near-infrared hyperspectral imaging," Artif. Organs **39**(8), 714–719 (2015).
18. D. Sakota, T. Murashige, R. Kosaka, T. Fujiwara, K. Ouchi, M. Nishida, and O. Maruyama, "Noninvasive optical imaging of thrombus formation in mechanical circulatory support devices," J. Biorheol. **30**(1), 6–12 (2016).
19. D. Sakota, R. Kosaka, M. Nishida, and O. Maruyama, "Optical aggregometry of red blood cells associated with the blood-clotting reaction in extracorporeal circulation support," J. Artif. Organs **19**(3), 241–248 (2016).
20. D. Sakota, T. Fujiwara, K. Ouchi, K. Kuwana, H. Yamazaki, and O. Maruyama, "Development of an optical detector of thrombus formation on the pivot bearing of a rotary blood pump," Artif. Organs **40**(9), 834–841 (2016).
21. T. Fujiwara, D. Sakota, K. Ohuchi, S. Endo, T. Tahara, T. Murashige, R. Kosaka, K. Oi, T. Mizuno, O. Maruyama, and H. Arai, "Optical dynamic analysis of thrombus inside a centrifugal blood pump during extracorporeal mechanical circulatory support in a porcine model," Artif. Organs **41**(10), 893–903 (2017).
22. T. Kume, T. Akasaka, T. Kawamoto, Y. Ogasawara, N. Watanabe, E. Toyota, Y. Neishi, R. Sukmawan, Y. Sadahira, and K. Yoshida, "Assessment of coronary arterial thrombus by optical coherence tomography," Am. J. Cardiol. **97**(12), 1713–1717 (2006).
23. H. Otake, J. Shite, J. Ako, T. Shinke, Y. Tanino, D. Ogasawara, T. Sawada, N. Miyoshi, H. Kato, B. K. Koo, Y. Honda, P. J. Fitzgerald, and K. Hirata, "Local determinants of thrombus formation following sirolimus-eluting stent implantation assessed by optical coherence tomography," JACC Cardiovasc. Interv. **2**(5), 459–466 (2009).
24. T. Yamane, R. Kosaka, M. Nishida, O. Maruyama, Y. Yamamoto, K. Kuwana, H. Kawamura, Y. Shiraishi, T. Yambe, Y. Sankai, and T. Tsutsui, "Enhancement of hemocompatibility of the MERA monopivot centrifugal pump: toward medium-term use," Artif. Organs **37**(2), 217–221 (2013).
25. T. Inoue, T. Kitamura, S. Torii, N. Hanayama, N. Oka, K. Itatani, T. Tomoyasu, Y. Irisawa, M. Shibata, H. Hayashi, M. Ono, and K. Miyaji, "Five-week use of a monopivot centrifugal blood pump as a right ventricular assist device in severe dilated cardiomyopathy," J. Artif. Organs **17**(1), 95–98 (2014).

1. Introduction

Thrombus formation remains a significant issue for patients requiring extracorporeal mechanical circulatory support (MCS) devices for therapies such as percutaneous cardiopulmonary support (PCPS), extracorporeal membrane oxygenation (ECMO), and as left and right ventricular assist devices (LVADs and RVADs) [1,2]. These extracorporeal MCS therapies have recently shown great potential for not only acute use but also mid-term use from several weeks to months as a bridge to an implantable artificial heart (bridge to bridge), bridge to transplantation, and bridge to recovery from severe cardiac failure [3–5]. To achieve safer MCS therapies, optimal anticoagulation management is required, so it is imperative for physicians to monitor the degree of anticoagulation in a patient's blood with utmost precision throughout the therapy. Conventional methods to quantify the anticoagulation level include activated clotting time (ACT), prothrombin time (PT), and activated partial thromboplastin time (APTT). However, due to the slow response time and qualitative nature of conventional methods, it is necessary to find faster and more accurate methods [6,7], especially for longer

Biomedical Optics EXPRESS

term use. Therefore, methods of real-time quantitative monitoring for the anticoagulation degree [8] or assessment of the blood-clotting reaction in MCS circuits [9–13] have been studied and developed. However, these methods are not yet suitable for practical clinical use, because they cannot be assembled where the thrombus formation actually occurs in MCS devices during actual clinical use. Although some ultrasound techniques to detect thrombi in flowing vessels have been used in clinical applications [14,15], our motivation is to achieve the earliest detection of a thrombus inside MCS devices before the thrombus is projected into a patient.

We have developed a real-time imaging and sensing method using visible and near-infrared light [16–21]. Our studies indicated that optically label-free and non-invasive techniques could detect blood clotting and thrombus formation from the very early to the end stages by detecting optically perceptive changes in the behavior of red blood cells (RBCs) surrounding the clotting area. Optical properties of the thrombogenic area significantly differ from the surrounding blood due to RBC aggregation/dis-aggregation when fibrin is generated, and the RBCs become trapped in or escape from the fibrin network, as shown in Fig. 1. The light scattering and absorption caused by fibrin is inconsiderable compared with those of RBCs. Therefore, our method does not directly detect the fibrin generation. The mechanism of how to detect and image thrombus formation in blood using visible and near-infrared light is the detection of the contrast in the RBC density between the clotting area and the surrounding blood. Such an optically detectable mechanism has been speculated in other studies, such as studies of optical coherence tomography [22,23]. We believe that an ultrasensitive real-time thrombus sensor that is able to detect very small thrombus formation at a non-projection hazard level will help physicians decide the optimal amount of anticoagulation agents.

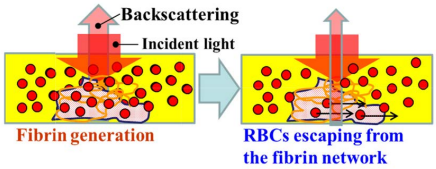

Fig. 1. Basic principle of how to detect thrombus formation in blood using visible and near-infrared light. The optical properties of a thrombus significantly differ from those of surrounding blood due to the difference in red blood cell (RBC) density caused by RBCs escaping from the fibrin network by blood flow.

In studies and development of MCS systems, the device design, the hemocompatible surface coating, and the materials used have mainly focused on antithrombogenicity. However, we are confident that our sensing technique will become a new approach to minimize the thrombus formation risk without changing the devices, as compared to other approaches. Our approach will especially contribute to extracorporeal MCS devices because they are inexpensively produced in large quantities. In addition, this study significantly contributes to the quantitative evaluation of antithrombogenicity. Our technique could become a fundamental technology for the development of more hemocompatible artificial organs and various MCS devices. This paper demonstrates that our sensor could be useful at the actual clinical level. We performed in vitro and animal experiments of extracorporeal circulation in pigs. We must note that no one has yet revealed the thrombogenic process in MCS devices. This study will contribute to the knowledge of anticoagulation management during MCS therapies.

The organization of the paper is as follows. To begin with, we show the developed thrombus sensor for the centrifugal blood pump actually used in Japan. Next, the layout of the experimental configuration and a description of the methodology are given. An in vitro experiment was conducted to investigate the optimal wavelength to achieve thrombus

Biomedical Optics EXPRESS

detection without being influenced by changes in the hematocrit (HCT) and the oxygen saturation (SaO_2). In addition, acute animal experiments using pigs were conducted three times to investigate the quantitative capability of the developed system. Then, the results and analysis show the clinical feasibility, and the novelty is presented. Finally, we state our conclusions.

2. Materials and methods

2.1 Developed optical thrombus sensor

The National Institute of Advanced Industrial Science and Technology (AIST) and Senko Medical Instruments Mfg. Co., Ltd. have developed a monopivot centrifugal blood pump (MERA HCF-MP23H) that has been available commercially in Japan since 2011. Besides being used during heart surgery, this pump can possibly be used for long-term PCPS or ECMO, and as an LVAD or RVAD. The pump without thrombus formation was evaluated over four weeks in an animal experiment using a goat. No anticoagulation occurred at an ACT from 180 to 200 s [24]. In clinical use, the pump was used for the RVAD at five weeks, and thrombus formation in the pump was not confirmed [25]. Then, we developed an optical thrombus sensor for the pump, as shown in Fig. 2, for wider and safer use, especially as a bridge to bridge and bridge to recovery pump without any changes in the pump design. The materials in contact with the blood are primarily polycarbonate, and the pivot bearing is a combination of a stainless steel (SUS) ball and a receptacle of ultra-high-molecular-weight polyethylene (UHMWPE). Although this pump has shown good hemocompatibility, the area of weakest antithrombogenicity is around the abuttal between the SUS ball and the secondary vanes of the impeller, and the contact point between the SUS ball and the UHMWPE. Therefore, a sensor was developed to monitor the thrombogenic process. The light guided by a plastic optical fiber (POF) with a core diameter of 200 μm is totally reflected in a vertical direction by a prism attached at the exit of the fiber, and the light is collimated by a hemisphere lens to aim it toward the center of the SUS ball. A total of five fibers (Optquest Co., Ltd., Saitama, Japan) for incident light or detection are embedded in the motor unit casing. However, in this study, only one pair of incident and detection POFs, located at 90 degrees from each other, were used for incident light and detection, respectively.

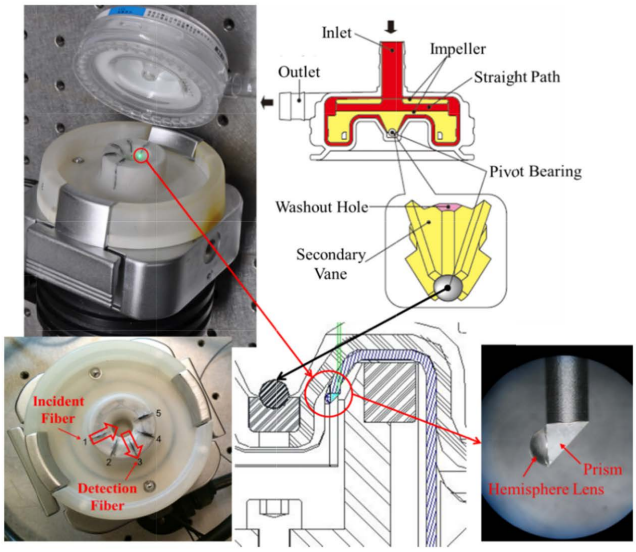

Fig. 2. Optical thrombus sensor for MERA centrifugal blood pump.

Biomedical Optics EXPRESS

Figure 3 shows the developed wavelength division multiplexing (WDM) module specially developed by Optquest Co., Ltd. Figure 3(a) shows the incident optical system to mix three wavelengths emitted from light-emitting diodes at 520, 650, and 810 nm. The respective power emitted from the POF was 220, 390, and 351 μW at 520, 650, and 810 nm. The incident POF has mixed light to irradiate the pivot through the surrounding blood flow. Then, the light was absorbed and scattered by the blood. The scattering light was guided by the detection POF. The detected lights were divided according to wavelength, as shown in Fig. 3(b), and received by an avalanche photodiode (APD). Figure 3(c) shows photos of the WDM in use. The analog signal from the APD was amplified by a DC strain amplifier (DSA-100A; Nissho-Electric-Works Co., Ltd., Tokyo, Japan). The amplified analog signal was converted to a digital signal at a 1 kHz sampling frequency using a data-acquisition system, and the data was analyzed by developed thrombus detection software installed in a personal computer.

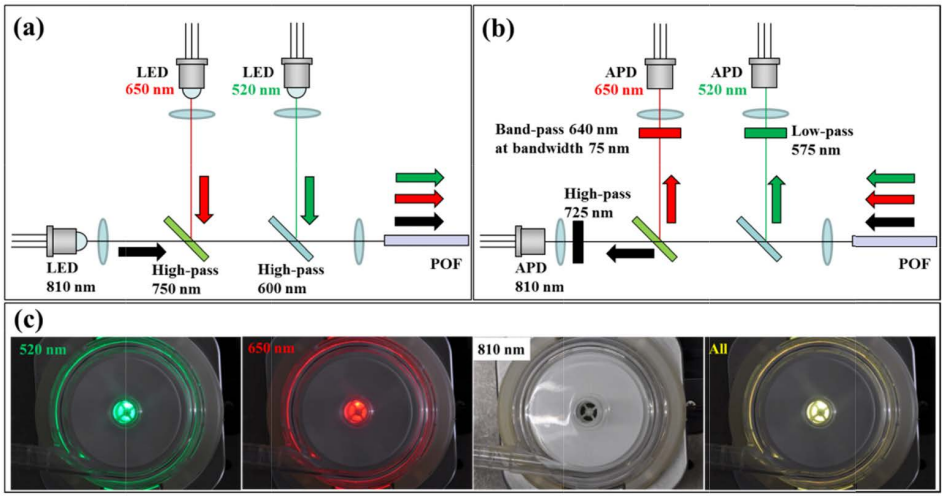

Fig. 3. Wavelength division multiplexing (WDM) module. (a) Incident system. (b) Detection system. (c) Photos of the WDM module in use.

Frequency analysis of the signal was conducted at the respective wavelengths to obtain the thrombus formation level (TFL) in the pivot bearing. In clinical use, the impeller of the MERA centrifugal blood pump is rotated at 1000 to 4000 rpm. We speculated that the thrombus formed on the pivot bearing must be rotated together with the impeller. Therefore, the rotational frequency components are significant. Short-term Fourier transform (STFT) was conducted using a Gaussian window of 1 s window width and 1 kHz sampling frequency. The left image in Fig. 4 shows a schematic of the back side of impeller and measurement of the light scattering around the rotating pivot. The incident light emitted from the incident POF is primarily scattered by RBCs around the pivot. Next, the light is further disturbed by four secondary vanes rotating with the impeller when the vanes are in the incident area. Otherwise, the light hits the SUS ball. The plot on the right in Fig. 4 shows the typical frequency spectrum obtained by STFT at 2400 rpm (40 Hz) when the impeller is rotated in porcine blood and when using the 810 nm wavelength. The component at four times the rotational frequency shows a stronger power than that of the rotational frequency. As a result, we defined TFL using the following equation:

$$\mathrm{TFL} = \mathrm{TFL}_t - \mathrm{TFL}_{t=0} = \left\{\frac{F(\omega)}{F(4\omega)}\right\}_t - \left\{\frac{F(\omega)}{F(4\omega)}\right\}_{t=0}. \quad (1)$$

Biomedical Optics EXPRESS

TFL_t is the TFL at the measurement time 't'. The start time of the measurement is t = 0. Therefore, TFL means the calibrated value at t = 0 to eliminate the individual differences of measurement that might be affected by the pump and the blood. F(ω) is the value after the STFT at frequency ω, which is the rotational frequency. So, F(4ω) is the value at 4 × ω.

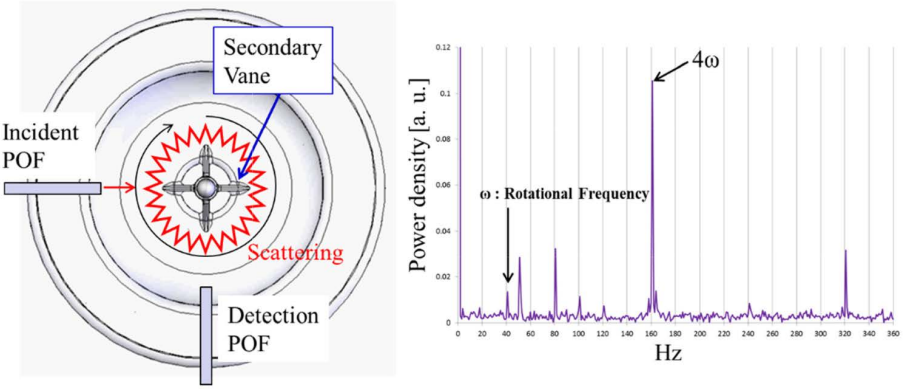

Fig. 4. Schematic of the back side of impeller and measurement, and the typical frequency spectrum of detected light intensity obtained by STFT at 2400 rpm (40 Hz) when the impeller is rotated in porcine blood and when using the 810 nm wavelength.

Both F(ω) and F(4ω) are definitely influenced by HCT and SaO_2, which are the main parameters related to light absorption and scattering in blood. However, the purpose of Eq. (1) is that F(ω) only changes when thrombus formation occurs around the rotating SUS ball, while F(4ω) does not change because thrombus formation does not occur on the secondary vanes. The situation is schematically shown in Fig. 5. Light scattering by secondary vanes fluctuates at four times the rotational frequency, and the vibration amplitude corresponds to F(4ω). Light scattering around the SUS ball fluctuates at the same frequency of the rotational speed, and the amplitude as shown at F(ω) will be significantly lower than that at F(4ω). Then, the TFL shown in Eq. (1) will be almost zero. However, when thrombus formation occurs around the SUS ball, a contrast in optical properties as shown in Fig. 1 will be generated. The effect will increase the amplitude of light scattering around the rotating SUS ball, as shown in Fig. 5. Here, F(4ω) will not change if the thrombus does not form on the four vanes. Finally, TFL will result in an increase.

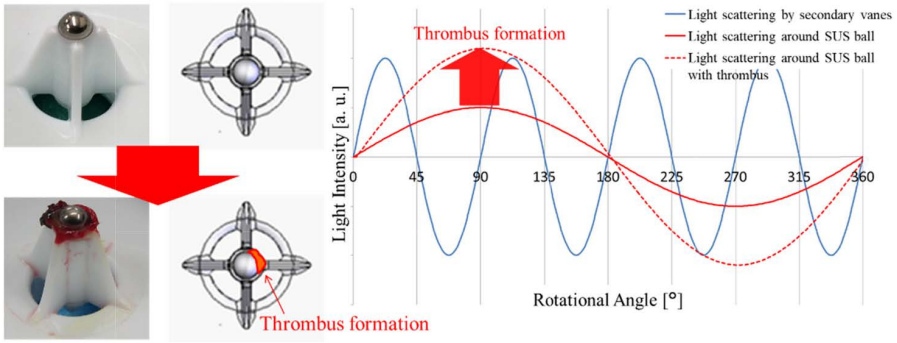

Fig. 5. Concept of thrombus formation level (TFL).

2.2 In vitro experiment

The change in Eq. (1) at each wavelength (520, 650, and 810 nm) with respect to HCT and SaO_2 was investigated in a closed-loop circuit that consisted of the MERA centrifugal blood

Biomedical Optics EXPRESS

pump, a polyvinyl chloride blood reservoir (special order product; Senko Medical Instrument Mfg. Co., Ltd., Tokyo, Japan), polyvinylchloride tubing (MERA Exceline-H 3/8 × 3/32; Senko Medical Instrument Mfg. Co., Ltd.), an oxygenator (HPO-23H-CP; Senko Medical Instrument Mfg. Co., Ltd.), and polycarbonate sampling connectors (MERA Exceline connectors 3/8 × 3/8; Senko Medical Instrument Mfg. Co., Ltd.). Fresh porcine blood obtained within 2 h from a local slaughterhouse was used. Anticoagulation of the blood was achieved by adding 100 cc of a 3.2% sodium citrate solution to 900 cc blood. The SaO_2 was altered by a mixture of gases, including O_2, N_2, and CO_2, through the oxygenator. The SaO_2 value was measured by a blood gas analyzer (ABL80-FLEX system; Radiometer, Ind., Tokyo, Japan). The HCT was altered by adding phosphate-buffered saline (PBS) solution from one of the sampling connectors.

2.3 Acute animal experiment of extracorporeal circulation designed as LVAD

Three Japanese specific pathogen-free pigs weighing approximately 80 kg were used in this study. This study was approved by the institutional animal care and use committees at AIST and Tokyo Medical and Dental University (application number 0170149A). Animals were anesthetized at the start of the experiment with a simultaneous injection of xylazine (2 mg/kg) and ketamine (20 mg/kg). Isoflurane was administered by inhalation and then intubation was performed. The arterial and venous lines from the ears of the pig were kept during the experiment. Extracellular fluid including various medications to stabilize the condition was infused from the venous lines. The arterial lines were used to monitor blood pressure and withdraw blood samples for hematological tests. An antibiotic agent (cefmetazole, 0.01 mg/kg) was injected several times intravenously before and during the operation. Lactated Ringer's solution (2 mg/kg/h) was administered as a maintenance transfusion. Inhalation anesthesia (isoflurane, 1%–3%) and intravenous anesthesia (propofol, 5 mg/kg/h) were used together during the operation and the experiment.

The operation for the left ventricular assist was performed with the animal in a lateral position. Left thoracotomy was performed through the sixth intercostal space, and the descending aorta was exposed. The pericardium was opened and the apex of the left ventricle was then exposed. An inflow cannula (22 Fr Optisite cannula) inserted into the apex of the left ventricle and an outflow cannula (18 Fr Optisite cannula) inserted into the descending aorta were connected to the extracorporeal circuit. The circuit consisted of the MERA centrifugal blood pump, polyvinyl chloride tube and polycarbonate connectors (MERA Exceline connectors 3/8 × 3/8; Senko Medical Instrument Mfg. Co., Ltd.). The length of the tube from the cannula to the pump was 2 m for both the inlet and outlet. The cannulae, tubes, and connectors, excluding the MERA centrifugal blood pump, were coated with heparin. The pump flow rate and the pump head pressure were continuously monitored in the same way as in the in vitro experiment. The mean flow rate was kept within the range from 1 to 2 L/min during the experiment. Chest wounds were closed after hemostasis was achieved. A photo of the experiment is shown in Fig. 6(a). Because the MERA HCF-MP23H has excellent antithrombogenicity, it is difficult to attain thrombus formation in the pump within several hours in an acute animal experiment. Therefore, to promote thrombus formation in the pivot area, a pump without heparin coating (MERA HCF-MP23) was used. In addition, an epoxy bonding agent was thinly applied on the gap between the SUS ball and the impeller, which is indicated by the area between the red lines shown in Fig. 6(b). After the epoxy had dried, the pumps were assembled and used in the experiments. Note that the experiments in this study does not show the actual antithrombogenicity of the MERA HCF-MP23. The epoxy was not placed on the center area of the SUS ball, because that area mechanically contacts the UHMWPE receptacle. In addition, the use of anticoagulation was limited to the timing of insertion of the inflow and outflow cannulae or the timing of the pump exchange. Then, a heparin bolus (120 U/kg) was infused to achieve an ACT over 200 s. After stable pump flow was confirmed, protamine (60 U/kg) was infused for approximately 15 min. As a result, the

Biomedical Optics EXPRESS

ACT value during optical monitoring was maintained at 100 ± 13 s (mean ± standard deviation).

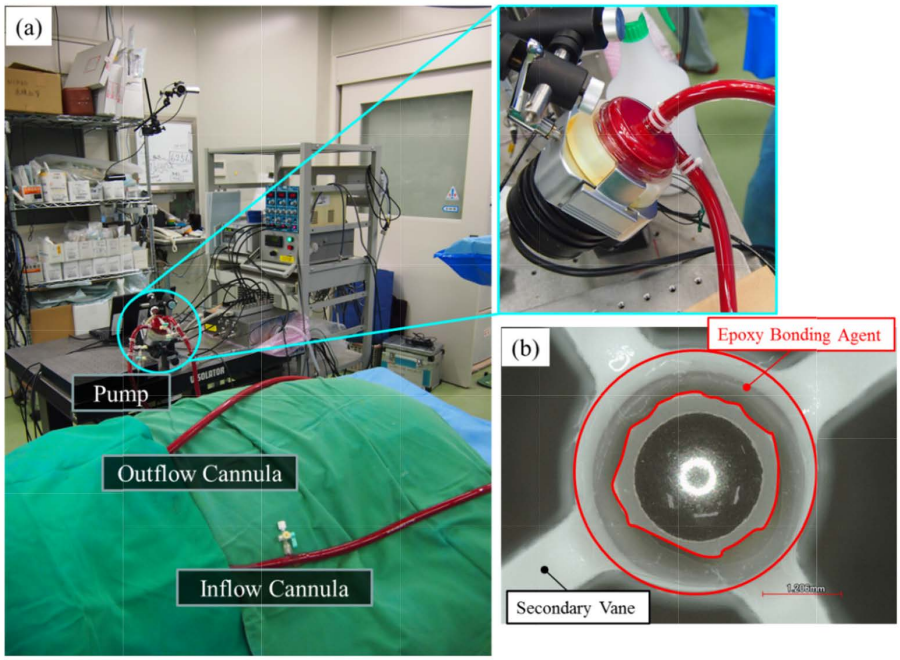

Fig. 6. (a) Photo of the animal experiment. (b) Pivot of the pump used in animal experiments. Epoxy bonding agent thinly put on the gap between the SUS ball and impeller to promote thrombus formation. Note that the experimental results in this study does not show the actual antithrombogenicity of the MERA HCF-MP23.

To quantify the thrombus formation area, a three-dimensional (3D) surface measurement system (VR-3000; KEYENCE Corp., Tokyo, Japan) was used. Figure 6(b) shows the view of the scanning area. After the pump exchange, the used pump was carefully taken apart to eject the impeller from the casing. 3D data from the top of the SUS ball to the secondary vane, including the thrombus, was obtained. The thrombus surface area was calculated using special software (VR-3000 G2 Series Software Ver.2.3.0.101; KEYENCE Corp.).

3. Results and discussion

3.1 Signal responses with respect to hematocrit and oxygen saturation

Figure 7(a) shows the TFL at 520 nm with respect to HCT and SaO_2. Clearly, the signal was not affected by either HCT or SaO_2. This result means that it is difficult to utilize blood sensing in this pump. Based on our previous studies [16,17,21], the mechanism of how to detect thrombus formation using visible and near-infrared light is shown in Fig. 1. The light at a wavelength that is strongly absorbed by hemoglobin responds to thrombus formation, because an optical change mainly occurs due to changes in the RBC density surrounding the clotting area. Therefore, light with a strong absorption will permit highly sensitive detection of changes in hemoglobin concentration with respect to thrombus formation. Although we expected that light at 520 nm could be used to detect thrombus formation, Fig. 7(a) indicates that the light absorption was too strong to utilize the thrombus sensor in this pump. The light hardly reached the SUS ball. The maximum blood thickness on the line of sight of the incident fiber is approximately 1.05 mm. Consequently, the light at 520 nm was inadequate as the light source for thrombus sensing in this pump.

Biomedical Optics EXPRESS

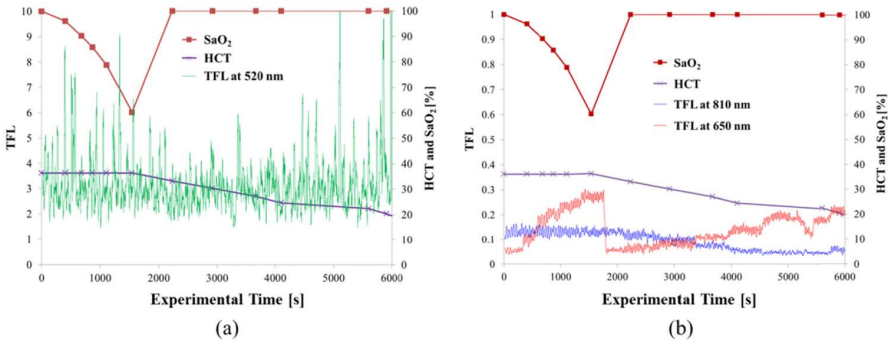

Fig. 7. (a) TFL at 520 nm with respect to HCT and SaO_2. (b) TFLs at 650 nm and 810 nm with respect to HCT and SaO_2.

In contrast, Fig. 7(b) shows that TFLs using both 650 nm and 810 nm lights responded to changes in HCT and SaO_2. However, the TFL at 650 nm strongly responded to SaO_2. The reason was the difference in the light absorption between oxy- and deoxyhemoglobin at 650 nm. The TFL at 810 nm is almost the isosbestic point and did not respond to SaO_2. As for HCT, when HCT decreases, the light direction is straighter and better illuminates the four secondary vanes. As a result, F(4ω) increased as the TFL decreased. However, the change in TFL was slight. The gradient was 0.004 [TFL/HCT].

3.2 Signal responses with respect to thrombus formation

In all of the experiments, no thrombus formed in the extracorporeal circuit, except for the pivot area of the pump, as shown in Fig. 8. This figure shows photos of the pumps after the animal experiments. The results of the three experiments were divided into group P1 (P1-1, P1-2, P1-3, P1-4), P2 (P2-1, P2-2, P2-3), and P3 (P3-1, P3-2, P3-3). In P2-2, thrombus formation is hardly seen. In only P2-3, thrombi formed in both the male and female bearings. The respective usage times of the pumps were P1 (152 min, 340 min, 142 min, 100 min), P2 (75 min, 76 min, 300 min, 176 min), and P3 (88 min, 47 min, 50 min).

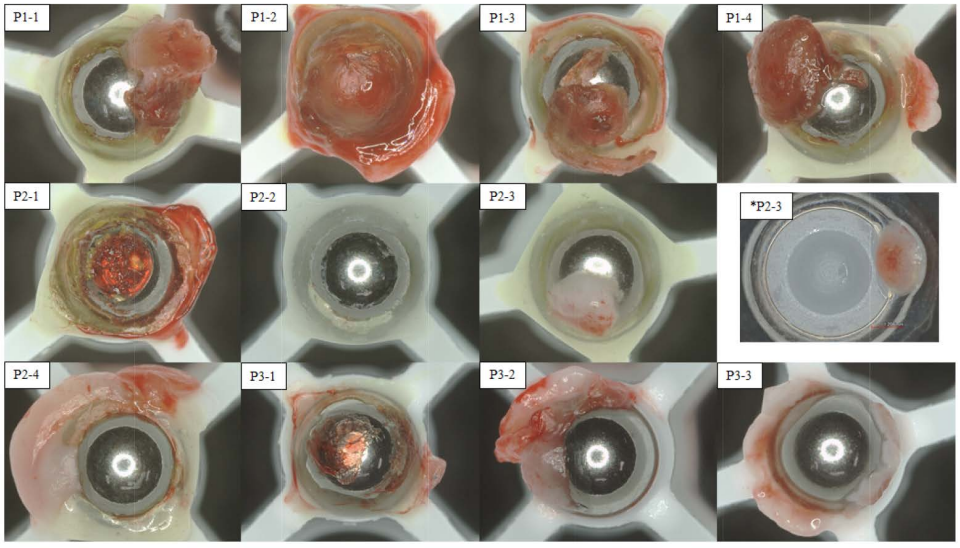

Fig. 8. Photos of pumps after the animal experiments. In P2-3, thrombi formed in both the male (P2-3) and female (*P2-3) bearings.

Biomedical Optics EXPRESS

Figure 9(a), 9(b), and 9(c) show the time trends of the TFL in each experiment using the light at 810 nm. In all cases, the TFL was kept constant at almost 0 in the early stage. However, after that, the TFL gradually increased. F(ω) increased because the thrombus, which has different optical properties compared with the surrounding blood, formed on the SUS ball rotating at the frequency of ω. In all experiments, the TFLs were dramatically changed compared with the SaO_2 and HCT changes shown in Fig. 7(b). The final values of TFL were P1 (1.0, 2.2, 1.65, 0.55), P2 (0.4, 0.13, 1.28), and P3 (0.36, 0.73, 0.5). In some cases, e.g., P1-3 and P2-4, the TFLs also decreased after showing the increasing trend.

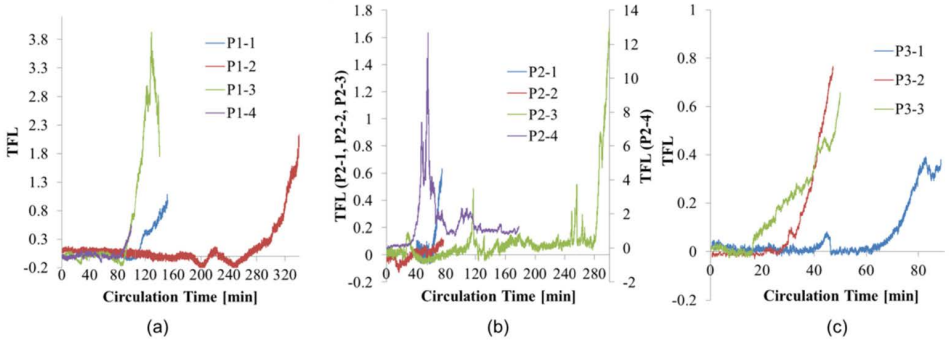

Fig. 9. Results of TFL monitoring after the animal experiments.

The obtained 3D data of the pivot and thrombus are shown in Fig. 10. The 3D thrombus surface area was calculated. The relationship between the results and the TFL is shown in Fig. 11. Here, the thrombus formation degree (TFD) was additionally calculated by dividing the thrombus formation area by the surface area of the SUS ball, which is 21.2 mm^2. The correlation coefficient was $R^2 = 0.878$, but the data of P2-3 was excluded because this case showed thrombus formation in the female bearing. The accuracy, or mean error rate, of the thrombus surface area and the TFD between the 3D surface measurement system and the developed thrombus sensor was estimated at 3.6 ± 2.3 mm^2 and 17 ± 13 [%], respectively. This result indicates the feasibility of quantitative monitoring of the thrombus growth process.

The gradient of the TFL with respect to the thrombus surface area was 0.117 [TFL/mm^2]. That value was large enough to ignore the influence of changes in the HCT. In the experiments, the HCT changed from 36.2 to 40.6 [%] at P1, and from pump start to end it changed from 31.5 to 39.4 [%] at P2, and 34.8 to 35.1 [%] at P3. Therefore, it was considered that the changes in TFL shown in Fig. 9 were caused by thrombus formation, and not changes in HCT. Consequently, the developed method could quantify thrombus formation using only 810 nm without the influence of SaO_2 and HCT. It should be noted that the quantitative performance for thrombus formation on the female bearing shown in *P2-3 was unknown. According to Eq. (1), it would be difficult to detect a motionless thrombus. However, thrombus formation on the female bearing hardly occurs in clinical observations. The P2-3 result might be due to the change in bearing performance by epoxy bonding.

According to Fig. 1, the light scattering changes with fibrin generation due to the changes in RBC density in the clotting area. As indicated in Fig. 11, the amplitude of light scattering around the SUS ball as obtained by F(ω) increases as the area increases. This can also be seen in Fig. 5. In this study, why the relationship between TFL and the thrombus surface area obtained by a 3D measurement system was very good has not been completely clarified yet. However, based on our previous studies [17,18], we speculate that the changes in light scattering with respect to thrombus formation are proportional to the reduction in the RBC density in the thrombus area shown in Fig. 1. Regardless, the developed sensor is able to quantify the thrombus growth process. We believe that the sensor could be utilized for

Biomedical Optics EXPRESS

selecting the proper time for pump exchange and the optimal amount of anticoagulation agents.

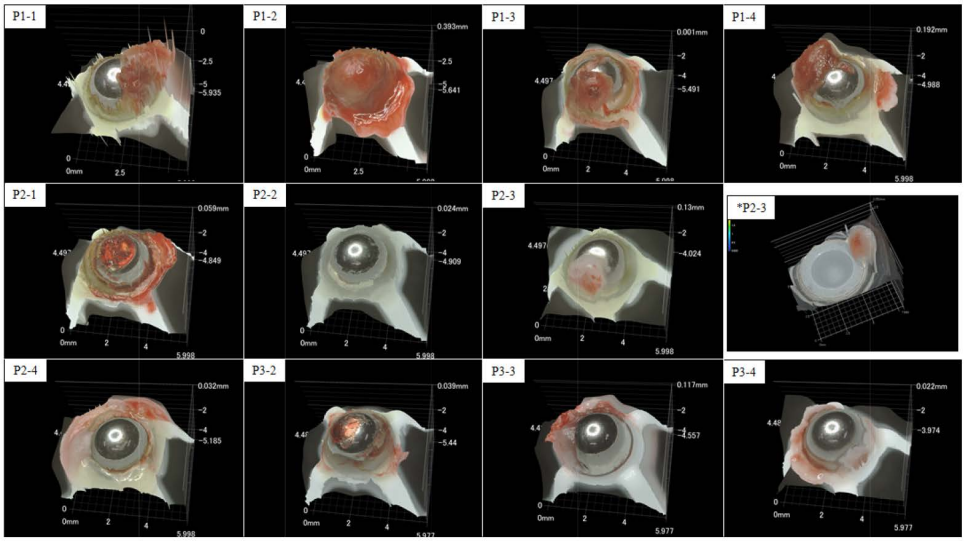

Fig. 10. 3D data of the pivot and thrombus. In P2-3, thrombi formed in both the male (P2-3) and female (*P2-3) bearings.

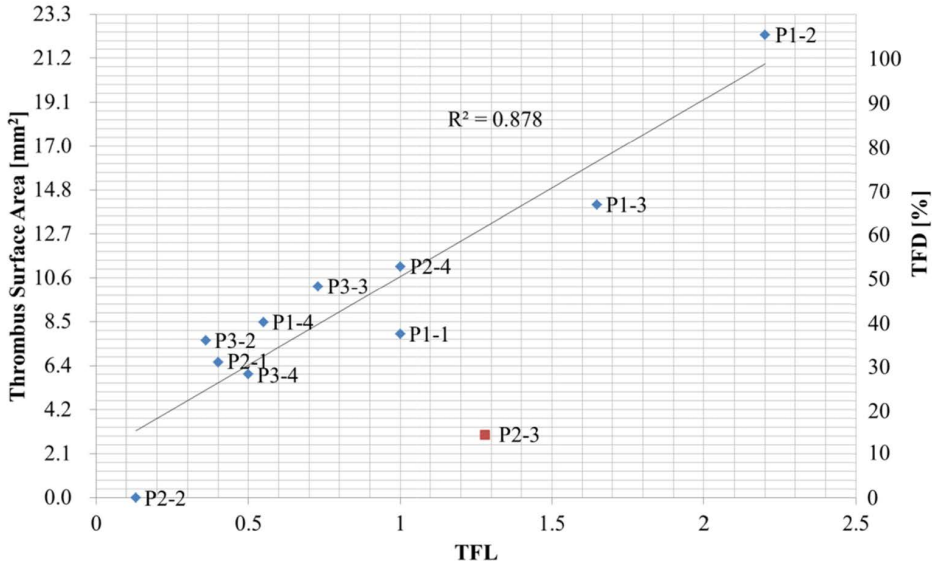

Fig. 11. Relationship between TFL and calculated thrombus surface area.

3.3 Future prospects: Using the obtained information

It is considered that the risk of disengagement of a thrombus at TFD < 100 [%] (TFL < 2.2) is quite low because the size of the thrombus is housed within the female bearing area. In other words, a larger thrombus might be disengaged by the washout flow generated by the secondary vanes. As shown in the results of P1-3 and P2-4 in Fig. 9, the decreasing trend of the increasing TFL indicates disengagement of the thrombus, so the results would serve as an

Biomedical Optics EXPRESS

alert of thrombus disengagement and the need to exchange the pump as soon as possible. Thus, the primary use of the thrombus sensor would be to inform physicians and co-medical personnel when the pump should be exchanged. As a higher-level use, it might be possible to stop further thrombus growth and to safely conduct thrombolysis by anticoagulation or thrombolytic therapy in the early stage, TFL < 1. That is the final goal for this research. The developed system can even detect the thrombus at a TFD less than 20 [%]. At this stage, it is expected that the small thrombus can be safely dissolved by increasing the anticoagulation agent or adding thrombolytics. Consequently, the physicians could continuously use the pump. It is known that the flexibility of conventional anticoagulation management has not been adequate. The optimal anticoagulation management should be the method in which thrombus formation in the device does not occur before the minimum ACT value. However, the risk is too high when the time of thrombus formation is unknown. Generally, we must set an extra ACT value, even if bleeding occurs to some extent. However, if real-time monitoring of thrombus formation is established, the risk can be dramatically reduced. As a result, physicians might be able to manage extracorporeal circulation therapies at low ACT values. The developed sensor might contribute not only to the reduction of thrombus risk but also to the reduction of bleeding.

For the development of MCS devices, real-time and quantitative monitoring of thrombus formation provides knowledge about the mechanism of the thrombogenic process in these devices and quantification of the hemocompatibility. The technology will contribute to the development of future artificial organs, as well as MCS and cardiovascular devices.

4. Conclusion

The developed optical thrombus sensor demonstrates the quantification of the thrombus surface area formed on a pivot bearing of a rotary blood pump. The present work demonstrates that a single wavelength measurement using 810 nm, which is a near-infrared and isosbestic wavelength for oxy- and deoxyhemoglobin, can be effective. Real-time and quantitative monitoring of thrombus formation in the pump in animal experiments was achieved. The accuracy was 3.6 ± 2.3 mm^2. The developed sensor could be useful for optimal anticoagulation management for long-term MCS.

Funding

JSPS KAKENHI (JP 16K01444) Saitama Prefecture.

Disclosures

Daisuke Sakota: Senko Medical Instrument Mfg. Co., Ltd. (F)